Investigation of antibacterial properties of TiN-Cu nanocoated nitinol archwires

Bojana Ilić *, Božana Petrović, Jelena Marinković, Jadranka Miletić Vukajlović, Momir Stevanović, Jelena Potočnik, Vukoman Jokanović

Posted Date: 16 August 2023

doi: 10.20944/preprints202308.1180.v1

Keywords: antibacterial activity; orthodontic archwires; Streptococcus mutans; nanocoatings

Article

Investigation of Antibacterial Properties of TiN-Cu Nanocoated Nitinol Archwires

Bojana Ilić [1,*], Božana Petrović [1], Jelena Marinković [1], Jadranka Miletić Vukajlović [1], Momir Stevanović [2], Jelena Potočnik [1] and Vukoman Jokanović [1,3]

[1] Vinca Institute of Nuclear Sciences, National Institute of the Republic of Serbia, University of Belgrade, Serbia
[2] Faculty of Medical Sciences, University of Kragujevac, Serbia
[3] Albos doo, Orahovačka 19, 11000 Belgrade, Serbia
* Correspondence: bcetenovic@vin.bg.ac.rs

Abstract: Background: The use of nitinol (NiTi) archwires in orthodontic treatment has expanded significantly due to unique mechanical properties. The greatest barrier to safe orthodontic treatment is chemically or microbiologically induced corrosion, resulting in Ni^{2+} release. The aim of this investigation was to enhance corrosion resistance and introduction antibacterial properties to NiTi archwire by coating them with TiN-Cu. Methods: NiTi archwires were coated with TiN-Cu using cathodic arc evaporation and direct current magnetron sputtering. The morphology of the sample was analyzed by FESEM and the chemical composition was assessed using EDS, XRD and FTIR. Inductively coupled plasma-optical emission spectrometry was used to estimate the ion release. Biocompatibility of samples was investigated using MTT test. Antibacterial activity was analyzed against *Streptococcus mutans* and *Streptococcus mitis*. Results: Physico-chemical characterization revealed well-designed coatings with the presence of TiN phase with incorporated Cu^{2+}. TiN-Cu coated archwires showed statistically lower Ni^{2+} release ($p<0.05$). Relative cell viability was the highest regarding 28-day eluates of TiN-Cu coated archwires ($p<0.05$). The most remarkable decrease in *Streptococcus mitis* concentrations was observed in case of TiN-Cu coated archwires ($p<0.05$). Conclusion: Taking into account biocompatibility and antibacterial tests, TiN-Cu coated archwires may be considered as a good candidate further clinical investigations.

Keywords: antibacterial activity; orthodontic archwires; *Streptococcus mutans*; nanocoatings

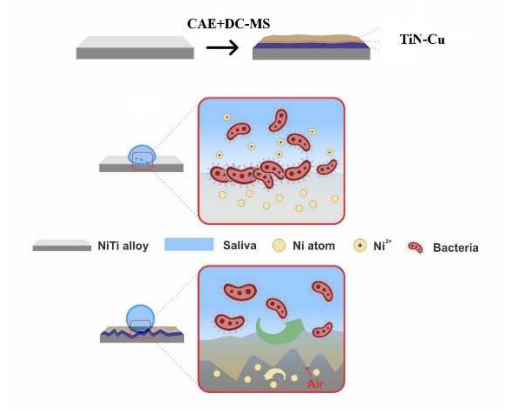

Introduction

The high prevalence of malocclusion in children is a consequence of genetic predisposition, bad habits, early loss of deciduous teeth as a result of dental caries, dental trauma, muscle dysfunctions or medications taken on daily bases [1]. The aim of orthodontic treatment (OT) is to accomplish and maintain an optimal occlusal relationship necessary to provide satisfying oral function and aesthetic appearance.

The use of nitinol (NiTi) archwires in orthodontic applications has expanded significantly due to unique mechanical properties such as shape memory effect (SME) and superelasticity (SE). Despite these favorable properties, the greatest barrier to safe OT is chemically or microbiologically induced corrosion of NiTi archwires. When placed in the oral environment, NiTi archwires are exposed to temperature and pH changes, the effect of food, drinks and oral health products abrasions, which all lead to the surface degradation and corrosion [2,3]. Corrosion of NiTi archwires result in Ni^{2+} release which acts on the local and systemic level, resulting in various health implications [4]. The synergy of different bacterial strains can affect the corrosion process directly (reduction and oxidation) or indirectly by creating metabolites that reduce pH value of the saliva. Locally, released Ni^{2+} induces gingival overgrowth and inflammation [5] significantly compromising the OT and leading to periodontitis. It also increases bacterial adhesion and biofilm formation [6] which provokes demineralization of the enamel and formation of white spot lesions (WSL) [7]. Additionally, significant increase of micronuclei in the buccal epithelial cells in children suggest its high genotoxicity and carcinogenicity [8,9].

Systemic effects of Ni^{2+} exposure should not be neglected as well, since Ni^{2+} is known as a strong immunologic sensitizer among 28.5% of the population, especially among children and adolescents [10,11]. Hypersensitivity, allergic contact dermatitis, and metal toxicity that increases urinary excretion of Ni^{2+} leading to renal tubular dysfunction are the most common adverse effects attributed to its exposure [8,12].

Considering health consequences, the necessity for developing novel material coating that would preserve mechanical properties of NiTi archwires, but decrease or eliminate Ni^{2+} release and improve biological properties is of a great importance. Well-satisfactory solution for the NiTi surface modification may be TiN as a very hard coating, well-adjusted to high mechanical loads that prevents metal ions leaching [13,14]. It was reported that TiN coating reduced corrosion rate of NiTi by 50% and Ni leaching by 35% in simulated blood [15]. Additional antibacterial properties can be achieved with introduction of copper (Cu) nanoparticles which possess the antibacterial effects against different bacterial strains [16]. It is estimated that the Cu content in the coatings by 2% wt is biocompatible, without damaging the liver, kidneys, and spleen [17].

Different methods of physical and chemical deposition processes have been used in order to modify the surface of NiTi archwires [18]. We hypothesize that by applying combined technologies of cathodic arc evaporation (CAE) and direct current magnetron sputtering (DC-MS) in the process of deposition of TiN coatings with Cu incorporation, Ni^{2+} release can be prevented, higher corrosion resistance and biocompatibility can be achieved with simultaneous introduction of antibacterial properties. Namely, CAE method involves thermal evaporation, where material is heated in vacuum until its vapor pressure becomes greater than the ambient pressure, and DS-MS implicates ion sputtering during which the high energy ions hits a solid, and incorporates inside of the thin layers of materials, used as a target. All these will obtain stable coatings and safe use of NiTi archwires during OT.

Based on the introductory information, the aim of this study was to investigate biocompatibility and antibacterial properties of TiN-Cu coated archwires in comparison to the NiTi and Stainless Steel (SS) archwires.

Materials and Methods

Deposition of the films

The TiN-Cu coatings were obtained on the surface of NiTi archwires (substrate, 0.018×0.025-*inch*) by the reactive CAE and DC-MS. The magnetron source for Cu sputtering was installed on one side of the vacuum chamber, while the circular titanium cathode for the arc evaporation was placed on the opposite side.

Prior to deposition, the substrate was ultrasonically cleaned in trichlorethylene, acetone, alcohol, and then dried with N gas. The argon (0.4 Pa, 5 min) was used for chamber cleaning while substrate bias was -700 V. During 5 min time, Ti interlayer was deposited on the substrate surface in the argon

 doi:10.20944/preprints202308.1180.v1

atmosphere (p=0.4 Pa) and substrate bias of -200 V. Then during 10 min time, TiN interlayer was deposited using nitrogen (p=0.4 Pa) and substrate bias of -200 V. In order to deposit TiN-Cu coatings, simultaneous DC-MS of Cu^{2+} and CAE of Ti^{2+} and in nitrogen atmosphere were used. During 30 min of deposition time, substrate bias was -150 V, Cu power density 0-5.2 W/cm^2, substrate temperature was 250 °C, rotation speed was 16 rpm with the distance (target-substrate) was 150 mm.

Physico-chemical characterization of the films

Field emission scanning electron microscopy with an energy dispersive X-ray spectrometer (FESEM-EDS, FEI SCIOS 2, Dual beam) was used to analyze the sample's morphology and composition. The micrographs were captured at an acceleration voltage of 6 kV. On the other hand, EDS measurement was performed at a voltage of 10 kV and 50 kx magnification. The sample was placed on a sample holder using double-sided adhesive carbon tape, after being sputter-coated with gold (Au) in order to increase conductivity.

Structural analysis of the coated NiTi wire was performed by the methods of X-ray diffraction (XRD) and Fourier transformed infrared spectroscopy (FTIR). XRD analysis was performed using Philips PW 1050 diffractometer with Cu-Kα1-2 lamp by collecting the data in the 2θ range from 15 to 80°, in steps of 0.055° and an exposure time of 2 sec per step. In order to implement FTIR analysis, spectrometer 380 Nicollet FTIR, Thermo Electron Corporation was used. FTIR spectra were taken in the spectral range from 4000 to 400 cm^{-1}.

Inductively Coupled Plasma- Optical Emission Spectroscopy

Investigated archwires were placed in Petri-dishes and immersed into 20 mL of ultrapure water (pH = 5.76 ± 0.51; conductivity of 0.055 mS/cm (Barnstead GenPure Pro; Thermo Scientific, Karlsruhe, Germany) or acidic solution (pH = 4.25 ± 0.51) for 7 days, 21 days and 28 days. The concentrations of Ni^{2+}, Ti^{2+} and Cu^{2+} in solution samples were measured by inductively coupled plasma-optical emission spectroscopy (ICP-OES) (n = 3). ICP-OES analysis was conducted by Thermo Scientific iCAP 6500 Duo ICP (Thermo Fisher Scientific, Cambridge, United Kingdom)

MTT Cytotoxicity Assay

The apical papilla of the healthy immature premolars extracted for orthodontic reasons (Ethics Committee 116-19-2/2020-000), was used for the isolation of stem cells from the apical papilla (*SCAP*s). Tissue fragments were washed twice in phosphate-buffered saline (PBS, Sigma-Aldrich, St. Louis, USA) and transferred into tissue culture dishes with 100 µL Dulbecco's Modified Eagle's Medium (DMEM/F12; Thermo Fisher Scientific, Inc., Valtam, USA), enriched with 20% fetal bovine serum (FBS; Thermo Fisher Scientific, Inc.) and 1% antibiotic/antifungal (ABAM; Thermo Fisher Scientific, Inc.). After 10 days of the incubation at 37^{o}C in a humidity 5% CO_2, fragments were removed. Once monolayered confluence was obtained, cells were washed with PBS and detached using 0.25% Trypsine (Sigma-Aldrich) and recultured. The characterization of cells was determined using the flow cytometry (Partec, *Munster* Germany) and conjugated monoclonal antibodies for membrane markers CD90 (FITC) (Life technologies, California, USA), CD73 (PB) (Sony Biotechnology, California, USA), CD105 (FITC) (Exbio, Prague, Czech Republic), CD34 (FITC) (Sony Biotechnology), CD45 (PE) (Exbio). In order to confirm mesenchymal potential of *SCAPs*, cells were cultured in different media (osteogenic/adipogenic/chondrogenic) (Miltenyi Biotec).

Investigated archwires (*0.018 × 0.025-inch*, Superelastic NiTi- OC Orthodontics, Stainless Steel- American Orthodontics, and TiN-Cu nanocoated archwires) were sterilized using UV and then immersed in Petri dishes (n=6) containing DMEM at 37°C in for 7 days, 21 days and 28 days (W/V ratio was 0.1 mg/mL), as recommended by the International Standard Organization (ISO) 10993-5. Prior to use the extracts were filtered to eliminate solid particles and stored at −20°C.

In order to perform MTT cytotoxicity test, cells were incubated with the culture medium (DMEM/F12) in 96-well plates. After 24 h of incubation, the culture medium was removed from well plates and 100 mL of 50% diluted and undiluted extracts were added per pool. After 24 h incubation

 doi:10.20944/preprints202308.1180.v1

at 37^{0}C in an atmosphere with 5% CO_2, 10 mL MTT solution (5 mg/mL in a phosphate buffer) was added per pool. After 4 h of incubation, 100 mL 10% sodium dodecylsulfate in 0.01 mol/L HCl was used per pool. The optical density was measured spectrophotometrically on enzyme-linked immunosorbent assay plate reader (Behring ELISA Processor II, Heidelberg, Germany) at a wavelength of 570 nm after 24h (n = 3). The metabolic activity of cell (% M) was determined following the formula:

$$\% \boldsymbol{M} = \frac{\boldsymbol{ODcell\ culture\ with\ samlpes - ODsamples\ without\ cell\ culture}}{\boldsymbol{ODcell\ culture\ without\ samples - ODcontrol\ medium}} \times \mathbf{100}$$

Bacterial adhesion and biofilm formation

Bacterial cultivation of *Streptococcus mutans* and *Streptococcus mitis* isolates was done by streaking of frozen stock cultures onto Mueller–Hinton agar (MHA, Oxoid) and incubation for 72 h at 37°C. Prior to experiment, single colonies of *Streptococcus mutans* and *Streptococcus mitis* were inoculated into Tryptone soya Broth (TSB, HiMedia, Mumbai, India) and grown overnight at 37°C. Cell suspensions were adjusted spectrophotometrically to an optical density OD_{600} of 0.2 (corresponding to $1x10^8$ CFU mL^{-1})

In order to test biofilm adhesion and to quantify adherent bacteria onto investigated archwires modified plate counting assay was used as following: under sterile conditions 1 cm of archwire was immersed in 1 ml of the bacterial suspension ($1x10^6$ CFU mL^{-1} in TSB enriched with 0,5% of glucose), being settled in each well of 24-well plate. After the 72 h of the incubation at 37°C, each archwire was removed from the well and placed into eppendorf tube containing 1 ml of sterile TSB. After the 15 min in ultrasonic bath (Sonorex, Bandelin Electronic, Berlin, Germany), and 2 min of the vortex, both being used to disturb biofilm settled on the wire, aliquots (100 µL) of concentrated or serially diluted (10^{-1} and 10^{-2}) medium were seeded on MHA. After the 48 h of incubation at 37°C, CFUs mL^{-1} were calculated. Two individual experiments in quadruplicate were performed.

Statistical Analysis

After conducting Kolmogorov-Smirnov test, statistical analysis was performed by using the repeated-measures analysis of variance (post hoc Tukey test). The level of significance was set at $p< 0.05$, and data were processed by using the statistical software IBM SPSS (IBM SPSS 20; IBM Corporation, Armonk, NY).

Results

FESEM

The morphology of the sample was analyzed by FESEM and the Figure 1 (a, b) displays micrographs taken at various magnifications. Figure 1a makes it abundantly evident that the deposited Cu is evenly distributed over the sample surface, while Figure 1b shows that the Cu particles have a combination of rounded and elongated morphologies, as well as their agglomerations. The results of the FESEM analysis revealed that the size of Cu particles is in the range from 20 nm to 130 nm.

Preprints (www.preprints.org) | NOT PEER-REVIEWED | Posted: 16 August 2023 doi:10.20944/preprints202308.1180.v1

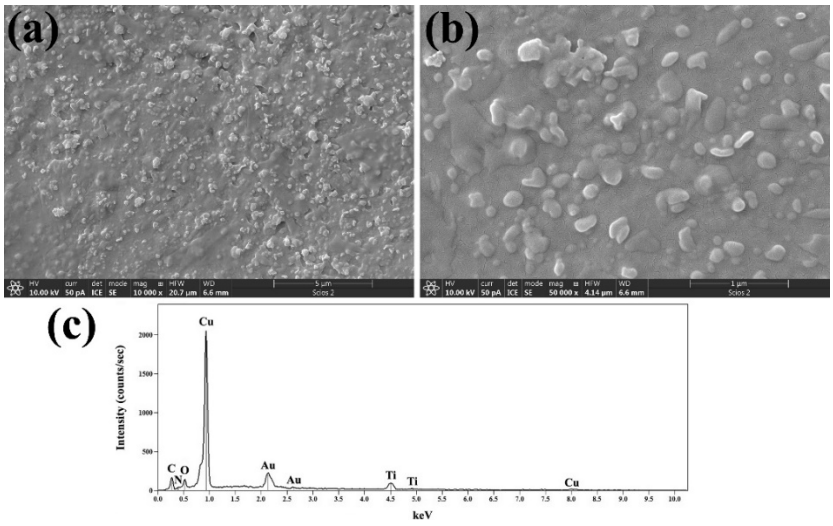

Figure 1. FESEM micrographs of the analyzed sample obtained at different magnifications:.(a) 5 kx and (b) 50 kx; (c) corresponding EDS spectrum.

In order to verify chemical composition, EDS analysis was also carried out, and the typical EDS spectrum, collected in the range of 0.1-10 keV, is shown in Figure 1c. The most intense peak belongs to copper (Cu), whereas the three smaller, lower-energy peaks are related with carbon (C), nitrogen (N), oxygen (O) and titanium (Ti). The presence of N and Ti peaks evidences deposited TiN layer. Aside from the previously mentioned peaks, the presence of a gold (Au) was also noticed, which originates from the sample's preparation for FESEM-EDS analysis.

XRD

XRD analysis confirmed the presence of the deposited TiN phase: planes (002) and (222) at the angles 42.46 and 77.64° (Figure 2). Presence of Cu is also evident at 43.49° (plane (111)) and by a small peak at 50.59° (plane (200) which is barely visible on the XRD pattern due to extremely high peak of TiN.

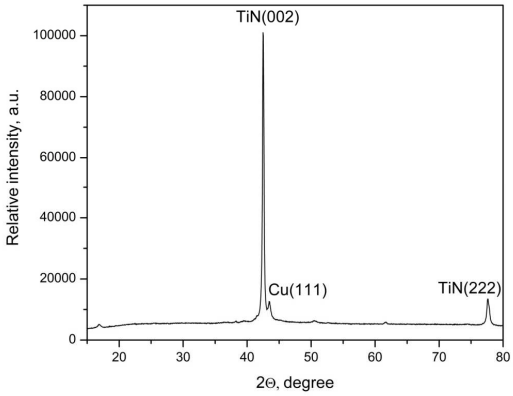

Figure 2. XRD pattern of the TiN-Cu nanocoated archwire.

FTIR

FTIR spectrum of the TiN-Cu coated archwire is shown in Figure 3. The bands at 3903, 3848, and 3732 and cm^{-1} can be ascribed to surface hydroxyl groups and absorbed water molecules, while bands at 3562 and 3281 cm^{-1} bands are attributed to the surface-absorbed water. The bands at 2923 and 2957 cm^{-1} can be attributed to OH radicals. The bands at 2635 and 2321 cm^{-1} can be assigned to overtone of carbonate impurities and adsorbed CO_2 on the surface thin films, while the band at 2173 cm^{-1} can be

Preprints (www.preprints.org) | NOT PEER-REVIEWED | Posted: 16 August 2023 doi:10.20944/preprints202308.1180.v1

assigned to the mode of parallel arranged CO oscillators adsorbed on fivefold coordinated Ti^{4+} sites on the main exposed TiO_2 surfaces. This effect can be explained as the progressive vanishing of the dynamic and static lateral interactions among the CO oscillators. This frequency is associated with isolated Ti^{4+} ···CO species. This band can be assigned to CO adsorbed coordinately to unsaturated Ti^{4+} sites on (001) faces, possessing a very low electrophilicity, and on some edges. The band at 1985 cm^{-1} indicates the formation of some new species in TiO_2 during oxygen or/and nitrogen doping. The band at 1660 cm^{-1} corresponds to bending vibrations of O–H and the bands at 1555, 1511 and 1456 cm^{-1} can be assigned to vibration of the CO^{2-} inside of the carbonate impurities. The bands around 1263 cm^{-1} are described as complex vibration involving CH, COH, and CCH motions. The band at 1158 cm^{-1} corresponds to C-C (ring) stretching vibration while the band at 1103 cm^{-1} can be assigned to the asymmetric stretching vibration correspond to the carbonyl group. The band at 1026 cm^{-1}, attributed to Ti-N stretching vibration evidences deposition of TiN phase. The band at 805 cm^{-1} can be assigned to the formation of multiply bonded TiO species, while the band at 546 cm^{-1} can be attributed to Ti-N stretching modes and Ti-O vibration in titanium oxides.

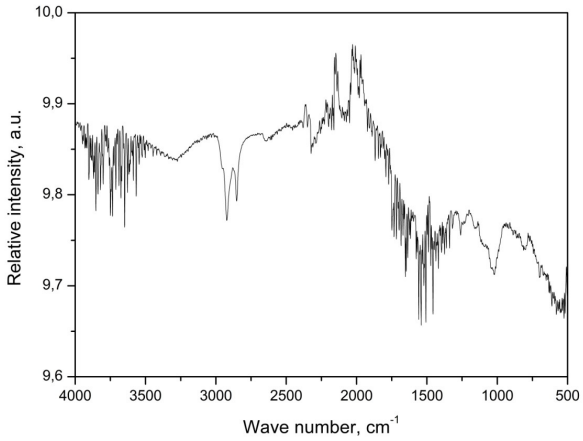

Figure 3. FTIR spectrum of the TiN-Cu nanocoated archwire.

Ion Release Measurements

Ion releases by investigated archwires into ultrapure water and acidic solution are presented in Table 1. Compared to NiTi and stainless steel, the TiN-Cu coated archwires showed statistically lower release of Ni^{2+} both in ultrapure water and acidic environment regarding all observation times ($p<0.05$). The release of Ni^{2+} increased during observation time in acidic conditions ($p<0.05$), contrary to neutral. The Ti^{2+} release was the highest regarding the NiTi archwires after 28 days in acidic conditions ($p<0.05$). The release of Ti^{2+} was constant during time in case of TiN-Cu coated archwires, contrary to NiTi. The release of Cu^{2+} was the highest regarding the TiN-Cu coated archwires after 7 days in neutral conditions ($p<0.05$), but decreased during time both in neutral and acidic conditions ($p<0.05$).

Preprints (www.preprints.org) | NOT PEER-REVIEWED | Posted: 16 August 2023 doi:10.20944/preprints202308.1180.v1

Table 1. Ion release into different solutions (ppb; mean value ± standard deviation).

	TiN-Cu coated archwire			NiTi archwire			SS archwire		
Ion	**7-day**	**21-day**	**28-day**	**7-day**	**21-day**	**28-day**	**7-day**	**21-day**	**28-day**
Ti water	2.8±0.2	3.8±0.1	4.1±0.1	3.1±0.2	3.0±0.1	3.1±0.1	1.6±.1	1.8±0.2	1.7±0.2
Ti acid	929±12	958±20	963±19	354±9	1144±23	1398±31	6.9±0.2	2.9±1.0	7.4±2.9
Ni water	6.1±0.1	6.1±0.1	1.7±0.1	33.9±0.1	21.0±0.1	19.7±0.2	3.5±0.1	3.7±0.3	3.7±0.2
Ni acid	59.9±0.8	1429±29	1443±21	555±5	1917±15	2129±20	49±2	75.7±3	111±2
Cu water	1210±0.8	1010±0.2	956±0.4	49.8±0.2	71.6±0.8	119±1.2	46.8±0.5	30.3±0.8	13±1.2
Cu acid	1020±1.2	961±0.4	879±0.7	59.3±0.4	78.2±0.2	128.1±0.1	82.4±0.2	40.1±0.1	25.6±1.0

MTT Analysis

The metabolic activity was the highest after 28-day extraction time in case of TiN-Cu coated archwires ($p < 0.05$), and slightly increased during the time regarding all investigated archwires (Figures 4 and 5). There were no statistically significant differences in metabolic activity between undiluted TiN-Cu coated samples and NiTi sample after 21 days of extraction ($p > 0.05$). Statistically significant differences between diluted eluates were observed at all observation time ($p < 0.05$).

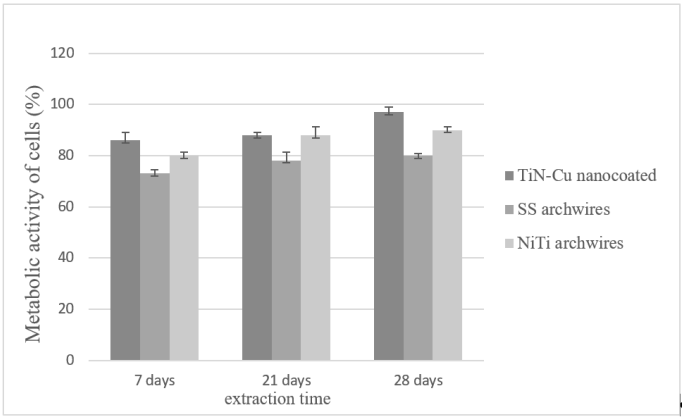

Figure 4. Metabolic activity of cells (%) after exposure to undiluted (100%) eluates of investigated archwires.

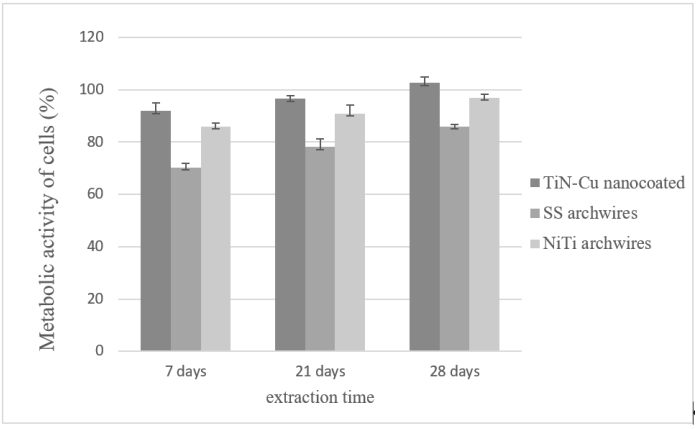

Figure 5. Metabolic activity of cells (%) after exposure to diluted (50%) eluates of investigated archwires.

Preprints (www.preprints.org) | NOT PEER-REVIEWED | Posted: 16 August 2023 doi:10.20944/preprints202308.1180.v1

Antibacterial Analysis

The final bacterial count for *Streptococcus mutans* and *Streptococcus mitis* regarding the all investigated archwires are presented in Table 2. The inhibitor effect of TiN-Cu coated NiTi archwires was observed against *Streptococcus mutans* and *Streptococcus mitis* ($p< 0.05$, Table 2). The lowest decrease in bacterial count was noticed regarding the SS archwires. The most remarkable decrease in *Streptococcus mitis* concentrations was observed in case of TiN-Cu coated archwires ($p< 0.05$). Though the control groups demonstrated decreases in bacterial count, the TiN-Cu coated archwires showed the most drastic decreases ($p< 0.05$).

Table 2. Final bacterial count for *Streptococcus mutans* and *Streptococcus mitis*.

	TiN-Cu coated archwires			**NiTi archwires**			**SS archwires**		
Bacteria	**Mean (cfu/mL)**	**SD**	**log**	**Mean (cfu/mL)**	**SD**	log	Mean (cfu/mL)	SD	log
S.mutans	$1.55x10^4$	$1.6x10^3$	4.19	$2.20x10^4$	$1.06x10^4$	4.29	$7.39x10^5$	$3.1x10^4$	5.87
S.mitis	$1.3x10^3$	$1.2x10^2$	3.08	$1.07x10^4$	$1.87x10^3$	3.75	$3.49x10^5$	$2.8x10^4$	5.54

Discussion

The coating of NiTi archwires in this study was performed by simultaneous application of two methods of physical vapor deposition, the method of CAE and DC-MS. As a method CAE is predominantly used for the deposition of high density nitride and some oxide coatings with improved adhesion. DC-MS shows numerous advantages over the other methods of physical vapor deposition due to its high rate and diverse metal/alloys coatings deposition on the surface of various materials with improved adhesion and excellent coverage. By applying the described technologies, we intended to modify the surface of NiTi archwires with multilayer coatings of high hardness, abrasion resistance and fine nanostructure, also providing the long-term chemical, thermal and environmental stability, which is essential for safe clinical use.

SEM characterization of designed coatings showed the nanostructure of Cu^{2+} particles (20 nm to 130 nm) that were evenly distributed on the TiN coating surface and well organized (combination of rounded and elongated morphologies, and their agglomerations). XRD, EDS and FTIR analyses confirmed the presence of TiN phase with incorporated Cu^{2+} ions which indicate that the films were adequately designed.

Bearing in mind the hypersensitivity to Ni^{2+}, especially in the female population, and although the released concentrations were lower than the permitted [19], the potential systemic effect or synergistic effects with other metal ions, must not be neglected. Ni^{2+} release was lower in the case of TiN-Cu coated archwires in both acidic and neutral environments. This result indicates that synthesized nanocoatings reduce Ni^{2+} release comparably to the other results [20,21]. It is well-known that titanium is biocompatible primarily due to the spontaneous formation of passivation layers, but increase in titanium release may be an indicator of the surface degradation and corrosion [22]. Although titanium is not considered as a metal that causes allergic reactions, there are studies showing it can cause type IV or type I hypersensitivity reactions in patients with dental implants [23]. In our study the release of titanium in acidic medium was constant during the observation time, comparably to other findings [20,24]. Also, its cumulative release was lower compared to NiTi archwires, leading to the conclusion that TiN-Cu coatings increased corrosion resistance of NiTi archwires which is crucial when biocompatibility is of great concern. As expected, the release of Cu^{2+} was the highest regarding the TiN-Cu coated archwires. Interestingly the release of Cu^{2+} was lower in acidic conditions compared to neutral, but remained below the maximum allowed levels [25]. In the present study, all investigated archwires exhibited favorable biocompatibility. The obtained results suggest that applied technologies provided well-designed nanocoatings with ion release rate non influencing its biocompatibility and cell viability. These findings are comparable to the previous results that revealed no cytotoxic effect of NiTi archwires [26,27].

 doi:10.20944/preprints202308.1180.v1

When introducing antibacterial properties to the NiTi archwires, the first strategy may be to create an antiadhesive surface protecting from biofilm formation. The second one is to design coatings with incorporated antibacterial substances that can also be released [28]. Antibacterial mechanism of metallic nanoparticles is based on their reaction with oxygen producing different types of reactive oxygen species (ROS). Leached metal ions may directly interact with bacterial cell wall or through electrostatic interactions (positively charged ions interact with the negatively charged membrane lipoproteins) resulting in the bacterial death. Furthermore, once metal nanoparticles enter bacterial cell, they may cause impairing damage to the DNA or disturb bacterial metabolism [28]. Different inorganic metals with antibacterial effects were used for introduction of antibacterial properties to NiTi archwires so far [28]. To the best of our knowledge, no previous studies investigated antibacterial properties of nano Cu incorporated in archwires coatings. Cu^{2+} is involved in the vital cellular functions, taking part in metabolic processes and enzymes activities [30]. The exact mechanism by which Cu^{2+} ions achieve their antibacterial potential has not been precisely determined, but it is believed that the synergism of all described models has its role [30].

The prevalence of WSL in the first six month of the fixed OT is 38% and 50% at the end of the treatment [7]. Therefore, applying antibacterial coatings overall complications requiring professional care and an annual cost will be reduced [31]. In order to assess antibacterial activity of TiN-Cu coatings, we have investigated adhesion of the *Streptococcus mutans* and *Streptococcus mitis* colonies to the wires. *Streptococcus mitis* is considered as primary colonizers of the dental biofilm forming up over 80% of the initial biofilm with other *Streptococci* [32]. *Streptococcus mutans* is one of the main causative of WSL enabling adhesion of other cariogenic bacteria by producing glucans while catalyzing sucrose [32]. Antibacterial tests indicate significant decrease in *Streptococcus mutas* and *Streptococcus mitis* counts, regarding both TiN-Cu nanocoated and NiTi archwires. Contrary, TiN coatings showed no reduction in *Streptococcus mutas* [33,34], which may indicate the importance of copper in the obtained results.

Conclusions

In the current investigation, TiN-Cu coatings obtained using combined technologies of cathodic arc evaporation and DC magnetron sputtering were evaluated in terms of biocompatibility, ion release and antibacterial properties. It was shown that designed TiN-Cu coatings on the surface of the NiTi archwires were stable both in neutral and acidic environment. Biocompatibility tests on *SCAP* cell lines showed safety of the investigated TiN-Cu coated NiTi archwires. The amount of Ni^{2+} release from the investigated TiN-Cu coated NiTi archwires are within the safety limit and significantly lower when compared to NiTi archwires. Antibacterial tests indicated decrease in *Streptococcus mutans* and *Streptococcus mitis* counts, so TiN-Cu nanocoated NiTi archwires may be considered as a good candidate further clinical investigations.

References

1. ADA American Dental Association. Oral Health and Well-Being in the United States. Available at: https://www.ada.org/en/science-research/health-policy-institute/oral-health-and-well-being.
2. Papadopoulou, K,; Eliades, T. Microbiologically-influenced corrosion of orthodontic alloys: a review of proposed mechanisms and effects. *Aust. Orthod. J.* **2009**, 25, 63-75.
3. Rincic Mlinaric, M,; Karlovic, S,; Ciganj, Z,; Pop Acev, D,; Pavlic, A,; Spalj, S. Oral antiseptics and nickel titanium alloys: mechanical and chemical effect of interaction. *Odontology*, **2019**, 107, 150-157.
4. Kulkarni, P,; Agrawal, S,; Bansal, A,; Jain, A,; Tiwari, U; Anand, A. Assessment of nickel release from various dental appliances used routinely in pediatric dentistry. *Indian. J. Dent.* **2016**, 7, 81-85.
5. Gursoy, UK,; Sokucu, O,; Uitto, VJ,; Aydin, A,; Demirer, S,; Toker, H,; Erdem, O,; Sayalet, A. The role of nickel accumulation and epithelial cell proliferation in orthodontic treatment- induced gingival overgrowth. *Eur. J. Orthod.* **2007**, 29, 555-558.
6. Amauri, JP,; Hwang, G,; Koo, H. Dynamics of bacterial population growth in biofilms resemble spatial and structural aspects of urbanization. *Nat. Commun.* **2020**, 11, 1354.
7. Lucchese, A,; Gherlone, E. Prevalence of white-spot lesions before and during orthodontic treatment with fixed appliances. *Eur. J. Orthod.* **2012**, 35, 664-668.

8. Morán-Martínez, J,; Monreal-de Luna, KD,; Betancourt-Martínez, ND,; Carranza-Rosales, P,; Contreras-Martínez, JG,; López-Meza, MC,; Rodríguez-Villarreal,; O. Genotoxicity in oral epithelial cells in children caused by nickel in metal crowns. *Genet. Mol. Res.* **2013**, 12, 3178-185.
9. Alp, G,; Çakmak, G,; Sert, M,; Burgaz, Y. Corrosion potential in artificial saliva and possible genotoxic and cytotoxic damage in buccal epithelial cells of patients who underwent Ni-Cr based porcelain-fused-to-metal fixed dental prostheses. *Mutat. Res. Genet. Toxicol. Environ. Mutagen.* **2018**, 827, 19-26.
10. Sfondrini, MF,; Cacciafiesta, V,; Maffia, E,; Scribante, A,; Alberti, G,; Biesuz, R,; Klersy, C. Nickel release form new conventional stainless steel, recycled, and nickel free orthodontic brackets: a in vitro study. *Am. J. Orthod. Dentofac. Orthop.* **2009**, 137, 809-815.
11. Biesiekierski, A,; Wang, J,; Gepreel, MA,; Wen, C. A newlook at biomedical Ti-based shape memory alloy. *Acta. Biomater.* **2012**, 8, 1661-1669.
12. Das, KK,; Reddy, R,; Bagoji, IB,; Das, S,; Bagali, S,; Mullur, L,; Khodnapur, JP,; Biradar, MS. Primary concept of nickel toxicity – an overview. *J. Basic. Clin. Physiol. Pharmacol.* **2018**, 30, 141-152.
13. Ikeda, D,; Ogawa, M,; Hara, Y,; Nishimura, Y,; Odusanya, O,; Azuma, K,; Satoshi Matsuda, S,; Yatsuzuka, M,; Murakami, A. Effect of nitrogen plasma-based ion implantation on joint prosthetic material. *Surf. Coat. Technol.* **2002**, 156, 301-305.
14. Weng, K,; Chen, Y,; Lin, T,; Wang, D. Characterization of Titanium Nitride Coatings Deposited by Metal Plasma Ion Pre-Implantation and Cathodic Arc Evaporation. *J. Nannosci. Nanotechnol.* **2009**, 9, 1127-1132.
15. Gill, P,; Musaramthota, V,; Munroe, N,; Datye, A,; Dua, R,; Haider, W,; McGoron, A,; Rokicki, R. Surface modification of Ni–Ti alloys for stent application after magnetoelectropolishing. *Mater. Sci. Eng. C. Mater. Biol. Appl.* **2015**, 50, 37-44.
16. Rau, JV,; Wu, VM,; Graziani, V,; Fadeeva, IV,; Fomin, AS,; Fosca, M,; Uskokovic, V. The Bone Building Blues: Self-hardening copper-doped calcium phosphate cement and its in vitro assessment against mammalian cells and bacteria. *Mater. Sci. Eng. C.* **2017**, 79, 270-279.
17. Chen, Z,; Meng, H,; Xing, G,; Chen, C,; Zhao, Y,; Jia, G,; Wang, T,; Yuan, H,; Ye, C,; Zhao, F,; Chai, Z,; Zhu, C,; Fang, X;, Ma, B,; Wan, L. Acute toxicological effects of copper nanoparticles in vivo. *Toxicol. Lett.* **2006**, 163, 109-120.
18. Tudose, IV,; Comanescu, F,; Pascariu, P,; Bucur, S,; Rusen, L,; Iacomi, F,; Koudoumas, E,; Suchea, M. Chapter 2 - Chemical and physical methods for multifunctional nanostructured interface fabrication, Editor(s): Valentina Dinca, Mirela Petruta Suchea, In Micro and Nano Technologies, Functional Nanostructured Interfaces for Environmental and Biomedical Applications, Elsevier, 2019, pp. 15-26
19. Nickel - Registration Dossier - ECHA. Available online: Registration Dossier - ECHA (europa.eu) (accessed on 9 June 2023).
20. Sugisawa, H,; Kitaura, H,; Ueda, K,; Kimura, K,; Ishida, M,; Ochi, Y,; Kishikawa, A,; Ogawa, S,; Takano-Yamamoto, T. Corrosion resistance and mechanical properties of titanium nitride plating on orthodontic wires. *Dent. Mater. J.* **2018**, 37, 286-292.
21. Ito, A,; Kitaura, H,; Sugisawa, H,; Noguchi, T,; Ohori, F,; Mizoguchi, I. Titanium nitride plating reduces nickel ion release from orthodontic wire. *Appl. Sci.* **2021**, *11*, 9745.
22. Bocchetta, P.; Chen, L.-Y.; Tardelli, J.D.C.; Reis, A.C.d.; Almeraya-Calderón, F.; Leo, P. Passive Layers and Corrosion Resistance of Biomedical Ti-6Al-4V and β-Ti Alloys. *Coatings* **2021**, *11*, 487.
23. Hosoki, M,; Nishigawa, K,; Miyamoto, Y,; Ohe, G,; Matsuka, Y. Allergic contact dermatitis caused by titanium screws and dental implants. *J. Prosthodont. Res.* **2016**, 60, 213-219.
24. Azizi, A,; Jamilian, A,; Nucci, F,; Kamali, Z,; Hosseinikhoo, N,; Perillo, L. Release of metal ions from round and rectangular NiTi wires. *Prog. Orthod.* **2016**, 17, 10.
25. Taylor, AA,; Tsuji, JS,; Garry, MR,; McArdle, ME,; Goodfellow, WL Jr,; Adams, WJ,; Menzie, CA. Critical Review of Exposure and Effects: Implications for Setting Regulatory Health Criteria for Ingested Copper. *Environ. Manage.* **2020**, 65, 131-159.
26. Jenko, M,; Godec, M,; Kocijan, A,; Rudolf, R,; Dolinar, D,; Ovsenik, M,; Gorensek, M,; Zaplotnik, R,; Mozetic, M. A new route to biocompatible Nitinol based on a rapid treatment with H2/O2 gaseous plasma. *Appl. Surf. Sci.* **2019**, 473, 976-984.
27. Rongo, R,; Valletta, R,; Bucci, R,; Rivieccio, V,; Galeotti, A,; Michelotti, A,; D'Antò, V. In vitro biocompatibility of nickel-titanium esthetic orthodontic archwires. *Angle. Orthod.* **2016**, 86, 789-795.
28. Godoy-Gallardo, M,; Eckhard, U,; Delgado, LM,; de Roo Puente, YJD,; Hoyos-Nogués, M,; Gil, FJ,; Perez, RA. Antibacterial approaches in tissue engineering using metal ions and nanoparticles: From mechanisms to applications. *Bioact. Mater.* **2021**, 6, 4470-4490.
29. Wang, N,; Yu, J,; Yan, J,; Hua, F. Recent advances in antibacterial coatings for orthodontic appliances. *Front. Bioeng. Biotechnol.* **2023**, 11, 1093926.
30. Ruiz, LM,; Libedinsky, A,; Elorza, AA. Role of Copper on Mitochondrial Function and Metabolism. *Front. Mol. Biosci.* **2021**, 8, 711227.
31. Ren, Y,; Jongsma, MA,; Mei, L,; Van Der Mei, HC,; Busscher, HJ. Orthodontic treatment with fixed appliances and biofilm formation--a potential public health threat? *Clin. Oral. Investig.* **2014**, 18, 1711-1718.

32. Kolenbrander, PE. Oral microbial communities: biofilms, interactions, and genetic systems. *Annu. Rev. Microbiol*. **2000**, 54, 413-437.
33. Teixeira, LP,; Gontijo, LC,; Franco Junior, AR,; Pereira, MF,; Schuenck, RP,, Malacarne-Zanon, J. Evaluation of antimicrobial potential and surface morphology in thin films of titanium nitride and calcium phosphate on orthodontic brackets. *Am. J. Orthod. Dentofac. Orthop.* **2021**, 160, 209-214.
34. Jabbari, YSA,; Fehrman, J,; Barnes, AC,; Zapf, AM,; Zinelis, S,; Berzins, DW. Titanium nitride and nitrogen ion implanted coated dental materials. *Coatings.* **2012**, 2, 160-178.